



THE UNIVERSITY *of* EDINBURGH

Edinburgh Research Explorer

A Dual Killing Strategy: Photocatalytic Generation of Singlet Oxygen with Concomitant Pt(IV) Prodrug Activation

Citation for published version:

Norman, D, Gambardella, A, Mount, A, Murray, A & Bradley, M 2019, 'A Dual Killing Strategy: Photocatalytic Generation of Singlet Oxygen with Concomitant Pt(IV) Prodrug Activation', *Angewandte Chemie International Edition*, vol. 58, no. 40, pp. 14189-14192. <https://doi.org/10.1002/anie.201908511>

Digital Object Identifier (DOI):

[10.1002/anie.201908511](https://doi.org/10.1002/anie.201908511)

Link:

[Link to publication record in Edinburgh Research Explorer](#)

Document Version:

Peer reviewed version

Published In:

Angewandte Chemie International Edition

General rights

Copyright for the publications made accessible via the Edinburgh Research Explorer is retained by the author(s) and / or other copyright owners and it is a condition of accessing these publications that users recognise and abide by the legal requirements associated with these rights.

Take down policy

The University of Edinburgh has made every reasonable effort to ensure that Edinburgh Research Explorer content complies with UK legislation. If you believe that the public display of this file breaches copyright please contact openaccess@ed.ac.uk providing details, and we will remove access to the work immediately and investigate your claim.



A Dual Killing Strategy — Photocatalytic Generation of Singlet Oxygen with Concomitant Pt(IV) Prodrug Activation

Daniel Norman,^[a] Alessia Gambardella^[a], Andrew Mount^[a], Alan Murray^[b] and Mark Bradley* ^[a]

Abstract: A Ruthenium-based mitochondrial-targeting photosensitiser that undergoes efficient cell uptake, enables the rapid catalytic conversion of Pt(IV) prodrugs into their active Pt(II) counterparts and drives the generation of singlet oxygen was designed. This duality drives two orthogonal killing mechanisms with cytotoxicity mediated with temporal and spatial control and was shown to elicit cell death of a panel of cancer cell lines including those showing oxaliplatin-resistance.

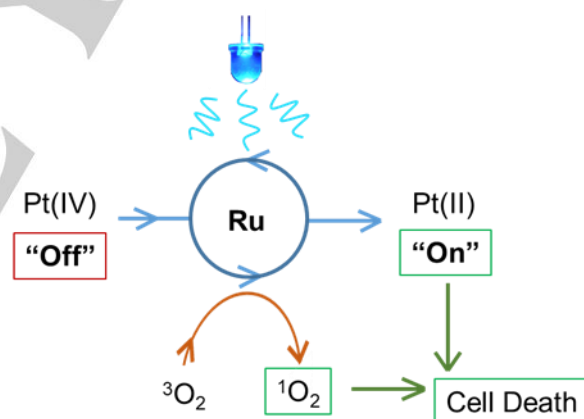
Photodynamic therapy (PDT) utilizes photosensitisers (PS) in combination with illumination to generate cytotoxic reactive oxygen species (ROS); primarily singlet oxygen ($^1\text{O}_2$)^[1]. As this only occurs in areas where light is focused, it enables spatially selective cytotoxic effects. Clinical applications of PDT include skin tumors^[2] and head and neck cancers^[3] as these are optically readily accessible.

Several porphyrin-based photosensitisers have been approved for clinical use including photofrin^[4], however it has serious side-effects in that patients may exhibit severe photosensitivity^[5], as well as non-specific damage to surrounding healthy tissue^[6]. Recently, a ruthenium-based photosensitiser, TLD-1433, completed Phase Ib clinical studies for bladder cancer treatment. This trial demonstrated the safety of this PS and also the utility of PDT at wavelengths outside of the “optimal window” with cancers that may not be considered optically accessible^[7].

A related therapeutic concept involves photo-activatable prodrugs, whereby irradiation generates a cytotoxic drug from an inert prodrug^[8]. Of relevance are the Pt-based photo-activatable prodrugs developed by Sadler et al^[9] where irradiation of a diazido-Pt(IV) complex gives rise to the cytotoxic Pt(II) counterpart, eliciting a dramatic increase in cytotoxic effect, ideal for photo-activated chemotherapy applications. Riboflavin has also been shown to be an effective photocatalyst for the conversion of Pt(IV) complexes to their cytotoxic Pt(II) counterparts^[10] (for other Pt(IV) approaches see review by Lippard et al^[11]).

Herein, we report the design, synthesis and evaluation of a photocatalytic Pt(IV) prodrug activation platform capable of

reducing Pt(IV) prodrugs while simultaneously generating singlet oxygen (Scheme 1). The Pt(IV) prodrugs were designed to be “bio-inert” prior to photochemically-induced reduction, while the photosensitiser (**PS-1**) was shown to be taken up rapidly by cells and localized in the mitochondria. Upon irradiation at 470 nm, the photosensitisers were capable of activating Pt(IV) prodrugs, while also causing significant oxidative damage to cells, thus affording a spatially- and temporally-controlled cytotoxic effect. The ability of this Pt(IV) prodrug activation system to overcome drug resistance was explored. While the commercial photosensitiser, Ru(bpy)₃Cl₂, was found to be capable of reducing Pt(IV) species, it had limited cell uptake. Therefore, a derivative, **PS-1**, was synthesized by addition of 1,3,3-trimethyl-2-methyleneindoline to 4-formylphenyl boronic acid (Scheme 2), followed by Suzuki-Miyaura coupling with 4-bromo-2,2'-bipyridine to afford the desired ligand that was treated with Ru(bpy)₂Cl₂ with replacement of the chloro ligands driven by microwave heating.



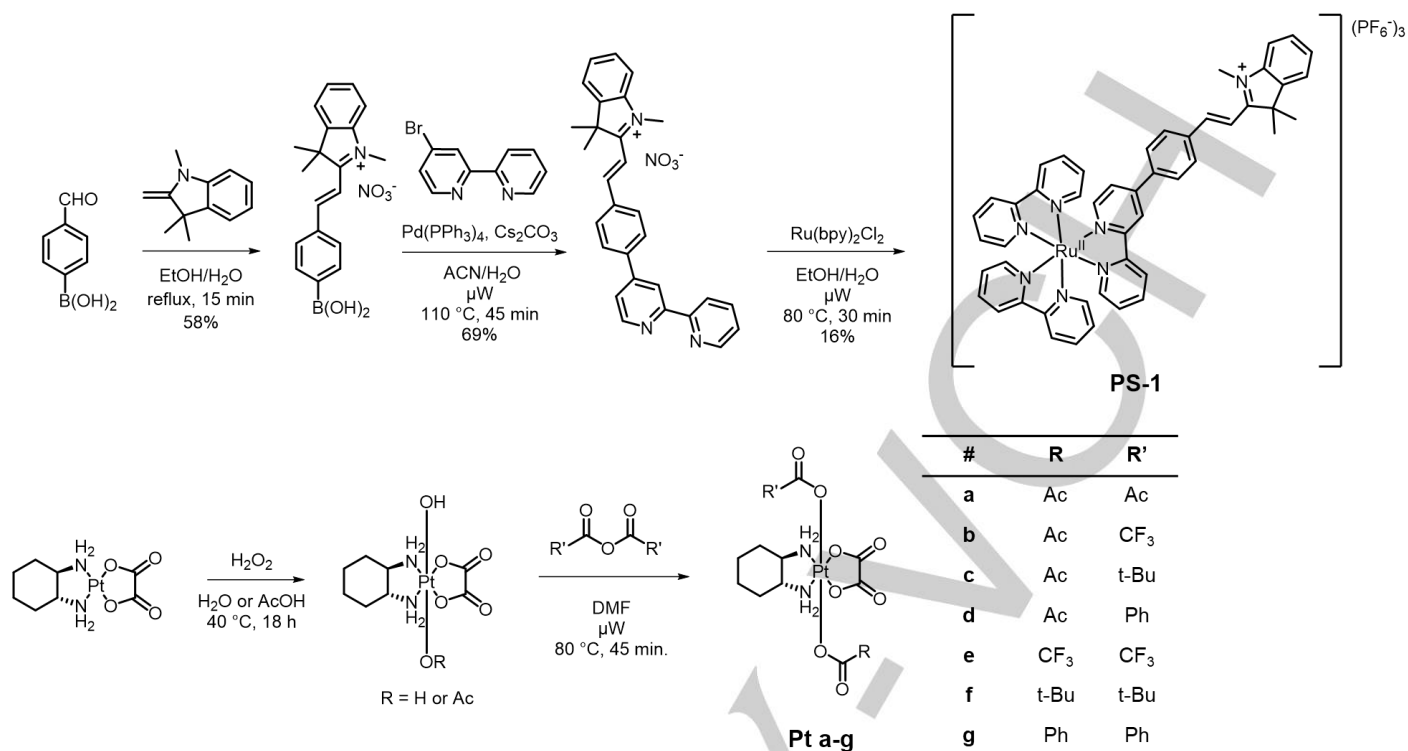
Scheme 1. Representation of the photocatalytic conversion of Pt(IV) prodrugs to their active Pt(II) counterparts by a Ru(II) photocatalyst with simultaneous $^1\text{O}_2$ generation.

Ruthenium-based photosensitisers generally display characteristic light absorption profiles^[12] due to ligand-to-ligand ($\pi\text{-}\pi^*$) and metal-to-ligand ($d\pi\text{-}\pi^*$) charge transfer bands and these were observed for **PS-1** (Figure S1). The singlet oxygen quantum yield of **PS-1** was quantified by the Singlet Oxygen Sensor Green (SOSG) assay^[13] and found to be 0.72 (compared to 0.88 for Ru(bpy)₃Cl₂^[14]) (Figure S2). In the presence of a Pt(IV) complex (**Pt-c**), the quantum yield reduced to 0.37. The photo-activation of the Pt(IV) species was desired to occur intracellularly so cellular uptake of **PS-1** was determined by ICP-MS. **PS-1** was observed to be taken up well by all three cell lines used, with 62–90% of the compound added to the culture media taken up into the cells after 4 h (see Table 1). The high cellular uptake of **PS-1** attributed to the positively charged indoline moiety and the lipophilic nature of the ligands, facilitating passage across the

[a] Dr. D. J. Norman, Ms. A. Gambardella Prof. A. R. Mount, Prof. M. Bradley
EaStChem School of Chemistry
University of Edinburgh
David Brewster Road, Edinburgh
E-mail: mark.bradley@ed.ac.uk

[b] Prof. A. F. Murray
School of Engineering
University of Edinburgh
Mayfield Rd, Edinburgh

Supporting information for this article is given via a link at the end of the document.



Scheme 2. Synthesis of the photocatalyst **PS-1** and the Pt(IV) prodrugs **Pt-a** to **Pt-g**.

negatively charged cell membrane; a feature that can be accentuated in cancer cells [15]. The stability of **PS-1** in complex media was demonstrated by incubation in 10% FBS in DMEM (Figure S3).

The ability of **PS-1** to elicit cell death upon illumination of light was confirmed in SKOV-3-wt cells (Figure S4). In the dark, **PS-1** has negligible effects on cell viability whereas when illuminated it generates cytotoxic reactive oxygen species (IC₅₀: 17 μ M).

To identify a "bio-inert" Pt(IV) prodrug, a series of symmetrical and non-symmetrical Pt(IV) complexes, **Pt-a** to **Pt-g**, were synthesized using standard conditions and screened against biological reductants to identify Pt(IV) prodrugs that were resistant to the biological reductants glutathione (GSH) and ascorbic acid (AsA) (Figure S5).

The non-symmetrical Pt(IV) complexes carrying an axial acetate ligand and either *tert*-butanoate or benzoate axial ligands (**Pt-c** and **Pt-d**) were stable to reduction by glutathione or ascorbic acid. Symmetrical complexes with increased steric hindrance, (**Pt-f** and **Pt-g**) were ineffective at preventing reduction. Electron-withdrawing axial ligands, such as trifluoroacetate (**Pt-b** and **Pt-e**) were unstable towards biological reductants, presumably due to destabilisation of the Pt(IV) center as has been observed previously [16]. **Pt-e** has also previously been shown to hydrolyze in solution to **Pt-b** expediting further reduction [17]. Prior work correlating trends of physicochemical properties of Pt(IV), such as reduction potential or logP have shown possible links to biological stability or activity [18]. Analyses of the reduction potentials of **Pt-a** to **Pt-g**, showed that **Pt-c** had the highest reduction potential (-0.90 V) which may confer its stability towards biological reductants (Figure S6 and Table S5). However, this is not the only determinant factor as similar reduction potentials were observed

for **Pt-f** and **Pt-g** (-0.86 V and -0.74 V, respectively), which were not stable towards biological reductants.

The complex **Pt-d** exhibited low water solubility and was discontinued from further studies with **Pt-c** taken forwards. **Pt-c** was also found to be relatively stable in 10% FBS in DMEM, as measured by HPLC (Figure S7). The difference in cytotoxicity of **Pt-c** compared to the clinical drug, oxaliplatin (OxPt), was analysed in HCT116 and SKOV-3-wt cells, showing that **Pt-c** exhibited significantly reduced cytotoxicity compared to the parent drug with IC₅₀'s of 64 vrs 9 μ M for SKOV-3-wt and 97 vrs 6 μ M for HCT116 cells (Figure S8).

The cellular uptake of **Pt-c** (as quantified by ICP-MS, Table 1) showed much greater uptake of the Pt(IV) prodrug than of OxPt, as is commonly observed in comparisons of Pt(II) and Pt(IV) complex cell uptake, as the Pt(IV) oxidation state affords more substitution-inert complexes than Pt(II) complexes [19], thereby enabling passage into cells without degradation or attack by biomolecules. The increased lipophilicity may also be responsible for promoting cellular uptake, although trends between cLogP and cellular accumulation of Pt complexes are often poorly correlated [20].

The ability of **PS-1** to photocatalytically reduce the Pt(IV) prodrug **Pt-c** into OxPt was confirmed, as shown in Figure 1, with **Pt-c** reduced into OxPt by 2 mol% **PS-1** by illumination (λ = 470 nm, 0.58 mW.cm⁻²), with 88% conversion observed after 60 min of illumination (Figures S9-S11) with the conversion of **Pt-c** to OxPt also confirmed by NMR (Figure 1b and Figure S12).

To quantify the level of cell death brought on by photoactivation of **Pt-c** and the dual oxidative damage inflicted by **PS-1** SKOV-3-wt and HCT116 cell lines were incubated with **PS-1** and **Pt-c** and irradiated.

COMMUNICATION

Cells that did not undergo irradiation showed little cell death when incubated with either **PS-1** or **PS-1** with **Pt-c** (Figure 2b).

Whereas when **PS-1** was used in conjunction with illumination there was significantly reduced cell viability, due to the generation of $^1\text{O}_2$ and other reactive oxygen species. To verify this, the singlet oxygen generation in cells was measured by co-incubation of SOSG and the turn-on of fluorescence tracked over time (Figure S13).

The combination of **PS-1** and **Pt-c** with illumination demonstrated very high levels of light-mediated cytotoxicity in both SKOV-3-wt and HCT116 cell lines. Due to the high uptake of **PS-1** and the increased uptake of **Pt-c** compared to OxPt and the efficacy of the photocatalysed Pt(IV) prodrug activation, it was hypothesised that light-mediated photocatalytic activation of **Pt-c** may be able to overcome the acquired resistance to OxPt. To explore this, SKOV-3-wt cells were allowed to accrue resistance to oxaliplatin by sub-culturing in incremental doses of OxPt over 3 months (procedure in ESI). The IC_{50} for OxPt in wild-type SKOV-3 (SKOV-3-wt) cells was $8.8\text{ }\mu\text{M}$, which increased some 3-fold to $25\text{ }\mu\text{M}$ for the more resistant cells (SKOV-3-OxR). The Pt(IV) prodrug **Pt-c** again exhibited reduced cytotoxicity compared to its Pt(II) counterpart, OxPt, with IC_{50} values of 82 vs $25\text{ }\mu\text{M}$ in the SKOV-3-OxR cells.

Photocatalytic activation of **Pt-c** in SKOV-3-OxR cells elicited substantial cell death, albeit with a slightly diminished cytotoxic effect than in SKOV-3-wt. Harvesting of the cellular DNA was performed 24 h post-photocatalytic activation of **Pt-c** in SKOV-3-wt and SKOV-3-OxR cells with the Pt content of each analysed by ICP-MS. There was a marked increase in platinated DNA in SKOV-3-wt and SKOV-3-OxR cells when **PS-1** and **Pt-c** were utilised in conjunction with light irradiation compared to controls (Figure S14). Interestingly, there was a larger overall platinated DNA content for SKOV-3-OxR (acquired resistance to oxaliplatin) than with either OxPt or photocatalysed Pt(IV)-Pt(II) conversion compared to SKOV-3-wt i.e. naïve cells towards oxaliplatin. As the photosensitiser was found to primarily localize in the

Table 1. Cellular uptake of **PS-1** and **Pt-c** as measured by ICP-MS

Compound ^[a]	Cell Line	Cell Uptake (ng/10 ⁶ cells)[%] ^[b]
PS-1	SKOV-3-wt	275 ± 9 (90 ± 3%)
	SKOV-3-OxR	191 ± 3 (63 ± 1%)
	HCT116	190 ± 10 (63 ± 3%)
Pt-c	SKOV-3-wt	531 ± 20 (14 ± 0.5%)
	SKOV-3-OxR	384 ± 2 (10 ± 0.04%)
	HCT116	458 ± 12 (12 ± 0.3%)
OxPt	SKOV-3-wt	161 ± 11 (1 ± 0.9%)
	SKOV-3-OxR	150 ± 5 (1 ± 0.4%)
	HCT116	281 ± 10 (2 ± 0.8%)

[a] Cells were incubated with either **PS-1** ($1\text{ }\mu\text{M}$) or **Pt-c** ($20\text{ }\mu\text{M}$) for 4 h at 37°C ($n = 3$)

[b] % uptake calculated as proportion of the theoretical maximal uptake.

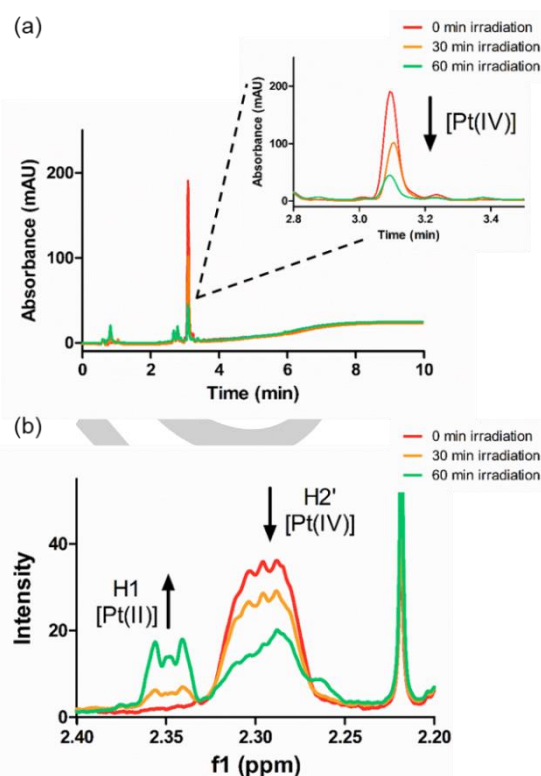


Figure 1. Analysis of the reduction of **Pt-c** by **PS-1**: (a) HPLC analysis of the photo-reduction ($\lambda = 470\text{ nm}$, $0.58\text{ mW}\cdot\text{cm}^{-2}$) of **Pt-c** ($50\text{ }\mu\text{M}$) by **PS-1** ($1\text{ }\mu\text{M}$) in PBS over time. (b) NMR analysis following the conversion of the Pt(IV) prodrug **Pt-c** ($100\text{ }\mu\text{M}$) into oxaliplatin (Pt(II)) in D_2O by monitoring the resonances correlating to the protons of the diaminocyclohexyl ligands.

mitochondria (Figure 2a and S15), cellular fractionation (into cytosol, mitochondrial and nuclear fractions) followed by ICP-MS analysis was used to probe the localization of the Pt(IV) prodrug in SKOV-3-wt cells (Figure S16). **Pt-c** was found mainly in the cytosolic fraction but was distributed throughout the cell, with slightly lower levels in the mitochondria and the nucleus. This ratio of distribution did not appear to be altered by the co-incubation of **PS-1**.

Finally, to explore the scope of this Pt(IV) prodrug activation system, the ability of two ruthenium-based photosensitisers to reduce three different Pt(IV) species was shown (Figure S17). TLD-1433, a photosensitiser currently under clinical investigation, was capable of reducing two oxaliplatin Pt(IV) species upon illumination of light. This was also shown to be possible with other platinum drugs, such as a Pt(IV) cisplatin derivative (**Cpt-Ac**). In conclusion, a photocatalytic platform for the simultaneous activation of Pt(IV) prodrugs and generation of singlet oxygen has been developed utilising a ruthenium-based photosensitiser. This system demonstrated excellent cytotoxic capabilities following illumination of cancer cell lines. The prodrug activation system overcame acquired Pt resistance in cells and demonstrated robustness in each of the cell lines used. The catalytic activation of Pt(IV) with concomitant singlet oxygen generation thus allows

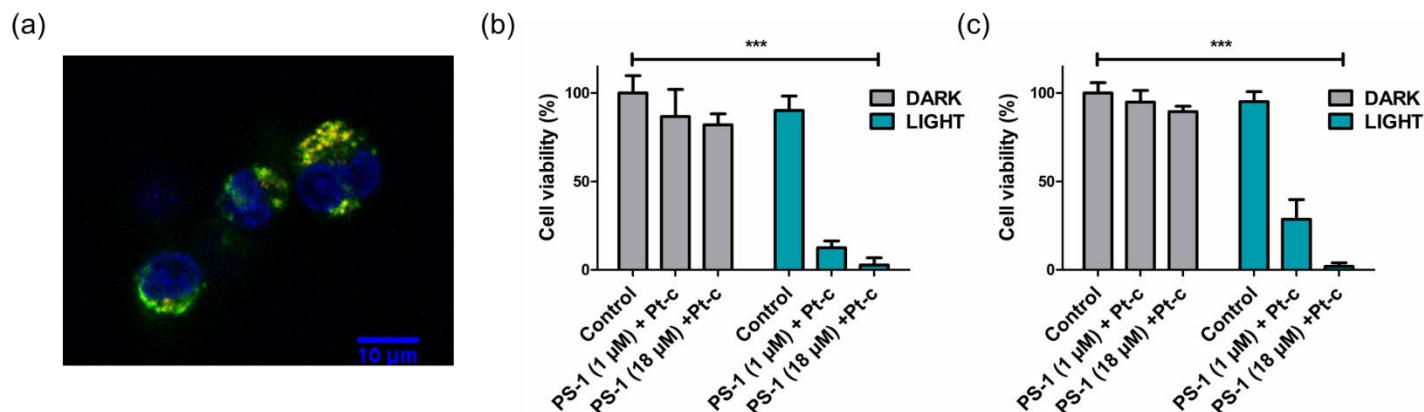


Figure 2. (a) Live-cell confocal microscopy showing co-localisation of **PS-1** (red) and MitoTracker (green) and nuclei (blue). Yellow shows overlap of green and red. Cell viability measured by Cell Titre Glo 2.0 for (b) SKOV-3-wt cells, (c) SKOV-3-OxR cells, with cells either in the dark or with illumination or untreated (control), with incubation with **PS-1** (1 μM) or incubation with **PS-1** (1 μM) with **Pt-c** (20 μM). The data represent the mean \pm S.D. *** $P < 0.001$ by one-way ANOVA with Tukey post-test

low dosing of photosensitiser which may help reduce phototoxicity-related side-effects. The composition of the photosensitiser will be further explored in terms of extending the absorption wavelength to more therapeutically applicable ranges through modification of the ligands and further enhancing the cancer-targeting capabilities of photocatalytic compounds that can be used for Pt(IV) prodrug activation

Acknowledgements

This work was supported by funding from University of Edinburgh and UK Engineering and Physical Sciences Research Council through the Implantable Microsystems for Personalised Anti-Cancer Therapy (IMPACT) programme grant (EPK034510/1). Data used within this publication can be accessed at:

Keywords: platinum • cancer • photocatalysis • prodrugs • anti-tumour agents

- [1] R. R. Allison, K. Moghissi, *Clinical Endoscopy* **2013**, *46*, 24–29.
- [2] a) P. G. Calzavara-Pinton, *Journal of Photochemistry and Photobiology B: Biology* **1995**, *29*, 53–57; b) P. Wolf, E. Rieger, H. Kerl, *Journal of the American Academy of Dermatology* **1993**, *28*, 17–21.
- [3] a) P. J. Lou, H. R. Jäger, L. Jones, T. Theodossy, S. G. Bown, C. Hopper, *British Journal of Cancer* **2004**, *91*, 441–446; b) K. F. M. Fan, C. Hopper, P. M. Speight, G. Buonaccorsi, A. J. MacRobert, S. G. Bown, *Cancer* **1996**, *78*, 1374–1383.
- [4] a) B. F. Overholt, C. J. Lightdale, K. K. Wang, M. I. Canto, S. Burdick, R. C. Haggitt, M. P. Bronner, S. L. Taylor, M. G. A. Grace, M. Depot, *Gastrointestinal Endoscopy* **2005**, *62*, 488–498; b) J. Gołąb, G. Wilczyński, R. Zagożdżon, T. Stokłosa, A. Dąbrowska, J. Rybczyńska, M. Wąsik, E. Machaj, T. Oldak, K. Kozar, R. Kamiński, A. Giermasz, A. Czajka, W. Lasek, W. Feleszko, M. Jakóbsiak, *British Journal Of Cancer* **2000**, *82*, 1485.
- [5] T. J. Dougherty, M. T. Cooper, T. S. Mang, *Lasers in Surgery and Medicine* **1990**, *10*, 485–488.
- [6] Z. Xiao, K. Brown, J. Tulip, R. B. Moore, *The Journal of Urology* **2003**, *169*, 352–356.
- [7] a) J. Fong, K. Kasimova, Y. Arenas, P. Kaspler, S. Lazic, A. Mandel, L. Lilge, *Photochemical & Photobiological Sciences* **2015**, *14*, 2014–2023; b) S. McFarland, A61P 35100 ed., **2013**.
- [8] a) P. Thapa, M. Li, M. Bio, P. Rajaputra, G. Nkepan, Y. Sun, S. Woo, Y. You, *Journal of Medicinal Chemistry* **2016**, *59*, 3204–3214; b) S. Sun, B. L. Oliveira, G. Jiménez-Osés, G. J. L. Bernardes, *Angewandte Chemie - International Edition* **2018**, *57*, 15832–15835; c) M. J. Hansen, F. M. Feringa, P. Kobauri, W. Szymanski, R. H. Medema, B. L. Feringa, *Journal of the American Chemical Society* **2018**, *140*, 13136–13141.
- [9] J. B. Patrick, S. M. Fiona, J. S. Peter, *Anti-Cancer Agents in Medicinal Chemistry* **2007**, *7*, 75–93.
- [10] S. Alonso-de Castro, E. Ruggiero, A. Ruiz-de-Angulo, E. Rezabal, J. C. Mareque-Rivas, X. Lopez, F. López-Gallego, L. Salassa, *Chemical Science* **2017**, *8*, 4619–4625.
- [11] T. C. Johnstone, K. Suntharalingam, S. J. Lippard, *Chemical Reviews* **2016**, *116*, 3436–3486.
- [12] a) S. Verma, P. Kar, A. Das, H. N. Ghosh, *Dalton Transactions* **2011**, *40*, 9765–9773; b) A. Juris, S. Campagna, V. Balzani, G. Gremaud, A. Von Zelewsky, *Inorganic Chemistry* **1988**, *27*, 3652–3655.
- [13] H. Lin, Y. Shen, D. Chen, L. Lin, B. Li, S. Xie, in *Photonics Asia 2010*, Vol. 7845, SPIE, **2010**, p. 6.
- [14] M. C. DeRosa, R. J. Crutchley, *Coordination Chemistry Reviews* **2002**, *233–234*, 351–371.
- [15] B. Chen, W. Le, Y. Wang, Z. Li, D. Wang, L. Ren, L. Lin, S. Cui, J. J. Hu, Y. Hu, P. Yang, R. C. Ewing, D. Shi, Z. Cui, *Theranostics* **2016**, *6*, 1887–1898.
- [16] S. Choi, C. Filotto, M. Bisanzo, S. Delaney, D. Lagasee, J. L. Whitworth, A. Jusko, C. Li, N. A. Wood, J. Willingham, A. Schwenker, K. Spaulding, *Inorganic Chemistry* **1998**, *37*, 2500–2504.
- [17] E. Wexselblatt, E. Yavin, D. Gibson, *Angewandte Chemie International Edition* **2013**, *52*, 6059–6062.
- [18] a) T. W. Hambley, A. R. Battle, G. B. Deacon, E. T. Lawrenz, G. D. Fallon, B. M. Gatehouse, L. K. Webster, S. Rainone, *Journal of Inorganic Biochemistry* **1999**, *77*, 3–12; b) P. Gramatica, E. Papa, M. Luini, E. Monti, M. B. Gariboldi, M. Ravera, E. Gabano, L. Gaviglio, D. Osella, *JBIC Journal of Biological Inorganic Chemistry* **2010**, *15*, 1157–1169.
- [19] J. Z. Zhang, E. Wexselblatt, T. W. Hambley, D. Gibson, *Chemical Communications* **2012**, *48*, 847–849.
- [20] R. Raveendran, J. P. Braude, E. Wexselblatt, V. Novohradsky, O. Stuchlikova, V. Brabec, V. Gandin, D. Gibson, *Chemical Science* **2016**, *7*, 2381–2391.

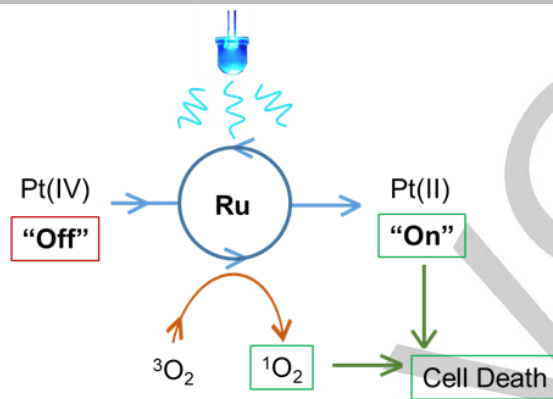
COMMUNICATION

Entry for the Table of Contents (Please choose one layout)

Layout 1:

COMMUNICATION

Text for Table of Contents



Author(s), Corresponding
Author(s)*

Page No. – Page No.

Title

Layout 2:

COMMUNICATION

((Insert TOC Graphic here))

Author(s), Corresponding Author(s)*

Page No. – Page No.

Title

Text for Table of Contents